PREPARATION OF BIOACTIVE NANOSTRUCTURE SCAFFOLD WITH IMPROVED COMPRESSIVE STRENGTH

F. TAVANGARIAN, R. EMADI

Department of Materials Engineering,
Isfahan University of Technology (IUT), Isfahan 84156-83111, Iran

E-mail: f_tavangarian@yahoo.com

Submitted September 27, 2010; accepted January 20, 2011

Keywords: Nanostructure materials, Bioactive glass, Ceramics, Hydroxyapatite, Scaffolds

Highly porous scaffolds with open structure are today the best candidates for bone substitution to ensure bone oxygenation and angiogenesis. In this study, we developed a new route to enhance the compressive strength of porous hydroxyapatite scaffold made of natural bone. Briefly, the spongy bone of an adult bovine was extracted, annealed, and coated by a nanostructure bioactive glass layer to be subsequently sintered at different temperatures. The apatite formation ability on the surfaces of the coated scaffolds was investigated by standard procedures. Our results showed that the scaffold and coating microstructure consisted of the grains smaller than 100 nm. These nanostructures improved the compressive strength and bioactivity of highly porous scaffold. The results showed that with increasing the sintering temperature, the compressive strength of scaffolds increased while their in vitro bioactivity decreased.

INTRODUCTION

Modern technologies constantly require materials and structures with special properties to achieve breath-taking innovations. This, in turn, requires constantly improving scientific and technological fabrication and working procedures.

Bone tissue engineering presents an alternative approach to the repair and regeneration of damaged bone tissue, avoiding the need for a permanent implant [1]. For this issue, three-dimensional biocompatible porous scaffolds with a highly interconnected porosity are designed. Porous scaffold ceramics were developed to prevent the loosening of implants. The growth of bone into the surface porosity provides a large interfacial area between the implant and its host. This method of attachment is often called biological fixation. It is capable of withstanding more complex stress states than other kinds of implants. Furthermore, porous scaffold implants allow cell migration, vascularization, and diffusion of nutrients. On the other hand, they form a mechanical bond via ingrowth of bone into the pores [2-4].

Macroporosity with pore sizes of 150-900 μm allows for nutrient supply and waste removal of cells grown on the scaffold. Microporosity with pores less than 10 μm is needed for capillary ingrowth and cell-matrix interactions [5-7]. The reduced mechanical strength of highly porous scaffolds, i.e. greater than 80% porosity HA scaffolds is a major drawback. Various efforts have been done for improvement of mechanical properties of highly porous ceramic scaffolds. Kim et al. [8] developed a highly porous HA (~86%) by polymer-sponge method with compressive strength of 0.21 MPa. In another work, these researchers [9] developed a composite coatings (Hydroxyapatite/poly(ε-caprolactone) on the porous hydroxyapatite and enhanced the compressive strength to 0.45. Tian et al. [10] improved compressive strength of porous HA (~82.46%) from 0.34 MPa to 0.8 MPa by developing PLLA onto the framework of sintered HA scaffold. Miao et al. [11] achieved the astounding results. They enhanced the compressive strength of porous HA (~86%) From 0.1 MPa to 2.39 MPa by impregnation of scaffold in PLGA–bioactive glass slurry and coating the struts. The aim of this paper is to develop a new scaffold with improved compression strength and high bioactivity. The results of this paper introduce a suitable candidate for load bearing applications and open new horizons in tissue engineering.

EXPERIMENTAL PROCEDURES

Preparation of scaffolds

The spongy bone of an adult bovine was extracted and then cut into rectangular samples of approximate size of 5×5×10 mm. The bone samples were annealed in an electric furnace, under ambient condition, at 1000 °C temperature for 2 h with a heating/cooling rate of 5°C/min.

This sample was named SH0. A sol-gel derived bioactive glass (coded as 58S) powder of a composition of 58 mol.% SiO_2, 38 mol.% CaO and 4 mol.% P_2O_5 was prepared through the hydrolysis and condensation of a mixed solution of tetraethylortosilicate (TEOS), triethylphosphate (TEP) and calcium nitrate tetrahydrate. These compositions have been investigated by Professor Hench's team at the Imperial College and have demonstrated high bioactivity in vitro [12, 13] and in vivo [14]. To prepare slurry, polyvinyl alcohol (PVA) was dissolved in distilled water (0.01 mol/L) and then 58S powder was added to solution, up to concentration of 15 wt.%. Each procedure was carried out under mild stirring using a magnetic stirrer for 2 h. The HA scaffolds with nearly same porosity and pore size were immersed in the prepared slurry and remained in it for 1 h. The coated scaffolds were then placed on a ceramic plate and dried at ambient temperature for at least 12 h. After drying, scaffolds were sintered at 800, 900 and 1000°C temperatures with 2 h holding time. These scaffolds were termed SH1, SH2, and SH3, respectively. The heating and cooling rates were 2 and 5°C/min, respectively. In vitro bioactivity of the obtained scaffolds was investigated by soaking the prepared samples in the simulated body fluid (SBF). This procedure has been widely used to prove the similarity between in vitro and in vivo behavior of certain bioceramic compositions. The SBF was prepared according to the standard procedure described by Kokubo et al [15]. The scaffolds were soaked in SBF (pH 7.40) at 37°C for 21 days. The ratio of solution volume to scaffold mass was 200 ml/g. After soaking, scaffolds were dried at 120°C for 1 day.

Characterization of scaffolds

The phase transformation of obtained scaffolds were investigated by X-ray diffractometry (XRD) analysis (Philips X'PERT MPD diffractometer with Cu Kα radiation - λ = 0.154056 nm). The XRD patterns were recorded in the 2θ range of 20-50° (step size 0.02° and time per step 1 s). The crystallite size of the synthesized scaffolds was calculated by the Scherrer's formula [16]. The morphology of the specimens was observed by scanning electron microscopy (SEM) (Philips XL30 at an acceleration voltage of 30 kV) coupled with energy dispersive spectrometer (EDS). The ability of Ca–P formation or Ca–P induction in vitro was semi-quantitatively compared by SEM examinations. The percentage of areas covered by Ca–P precipitation was evaluated from SEM micrographs for each type of sample. Image analysis method was used for measurement of coating grains and mean size of pores. The porosity of scaffolds was measured according to Archimedes principle [17]. The compressive strength of the scaffolds was measured using a universal testing machine (AG-400NL, Shimadzu Co., Japan) at a crosshead speed of 0.5 mm/min.

RESULTS AND DISCUSSION

Figure 1 shows the XRD patterns of scaffolds that sintered at different temperatures. All the XRD patterns obtained for the samples were in agreement with the stoichiometric HA characterized pattern (XRD JCPDS data file No. 9-432). The XRD patterns of coated scaffolds (SH1, SH2, and SH3) were almost similar and exhibited an increase in peak height and a decrease in peak width, thus indicating an increase in crystallinity and crystallite size. XRD analysis could not identify the coating material because of the amorphous state and low amount of the bioactive glass. As the sintering temperature of coated scaffolds increased to 1000°C, some new peaks could be detected. In SH3, both angular location and intensity of the peaks match the standard (XRD JCPDS data file No. 22-1318), which indicates that the crystalline phase is SiP_2O_7.

The crystallite size of the obtained scaffolds was calculated by the Scherrer's formula [16]. The Bragg reflection at (211) plane of HA was considered to calculate the crystallite size. The crystallites size of HA in SH0, SH1, SH2, and SH3 samples were about 68, 75, 82, and 94 nm, respectively.

Figure 2 shows the compressive strength and porosity of different samples. The porosity of samples varied in narrow range. It can be interpreted that coating was the thin layer and therefore had a minor effect on the porosity size. According to the Figure 2, as the sintering temperature increased to 1000 °C, the compressive strength of scaffolds enhanced from 0.22 to 1.49 MPa. This observation confirmed the finding of Clupper and Hench [18] that some crystallization occurs prior to significant viscous flow sintering in bioactive glasses.

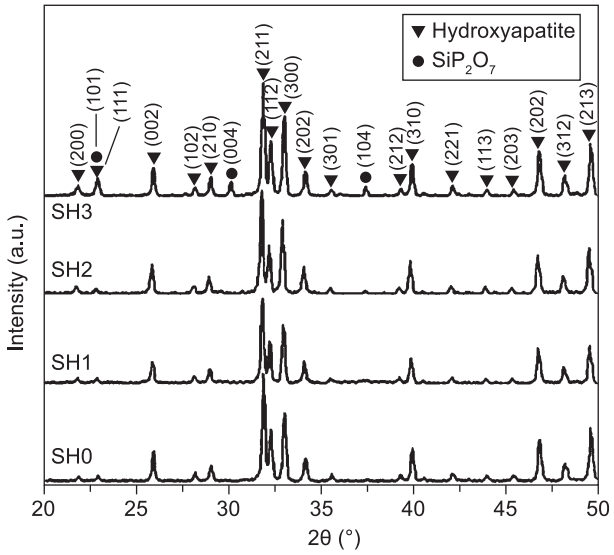

Figure 1. X-ray diffraction patterns of SH0, SH1, SH2 and SH3.

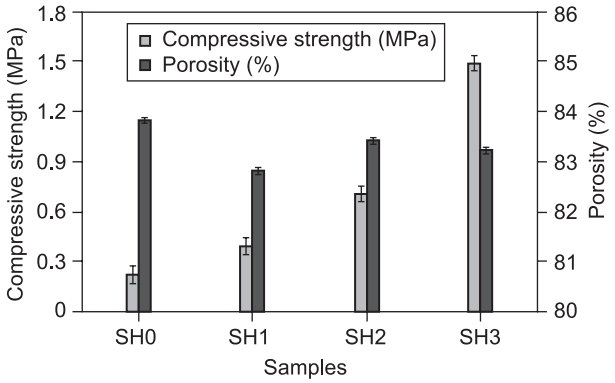

Figure 2. The compressive strength and porosity of different samples.

The typical macroporous network and surface morphology of SH3 are illustrated in Figure 3a. All scaffolds exhibited pore size ~800 μm and porosity of ~83%. The coating microstructure of SH3 is shown in Figures 3b and c. Fine crystalline grains range between 91 and 320 nm and micron size pores could be detected. Figure 3d exhibits the elemental analysis of coating material as well as strut surface. Silicon could be seen in the EDX pattern that confirmed the presence of bioactive glass on the struts of HA. The combination of densification and the presence of a crystalline phase in the struts of scaffolds sintered at 1000 °C are expected to lead to improved mechanical properties of these foams. As can be seen in Figure 2, SH1 and SH2 exhibited lower compressive strength than SH3 so it could be concluded that sintering temperatures of SH1 and SH2 were inadequate for the bonding of particles. Prepared scaffolds by this method are very similar to spongy bone as compared with reports on mechanical property and pore structure of cancellous bone [19, 20]. The compressive strength of spongy bone is in the range of 0.2-4 MPa. The measured compressive strength (0.39-1.49 MPa) of the present coated foams falls in this range so the present bioactive glass coated HA scaffolds possess such an appropriate mechanical competence. It is obvious that the present nanostructured bioactive glass coated HA foams (porosity: ~83%, compressive strength: 1.49 MPa) are in general stronger than the HA-based foams of similar porosities Moreover in this research polymeric materials are not used as a coating material.

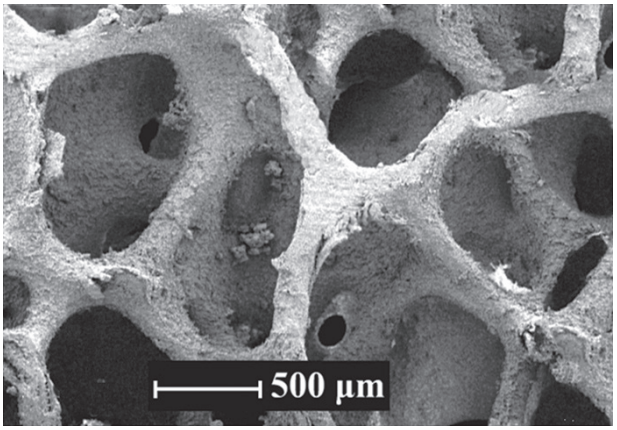

a) pore structure

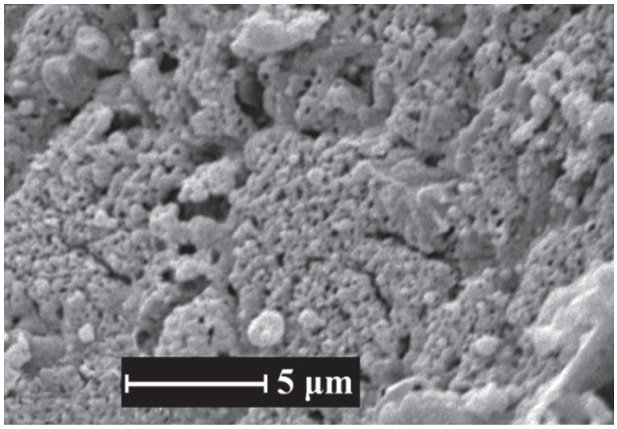

b) microstructure of strut

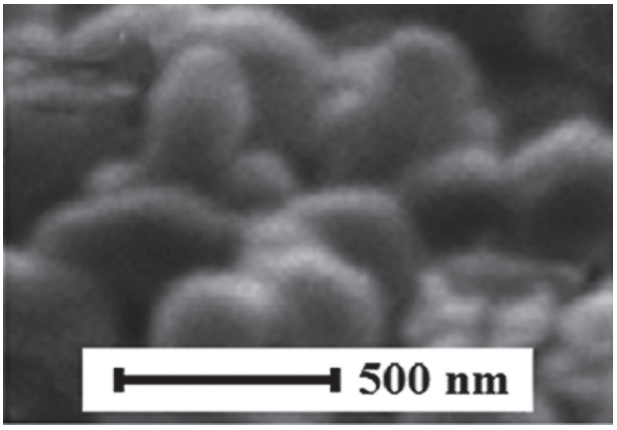

c) microstructure of coating at higher magnification (50000×)

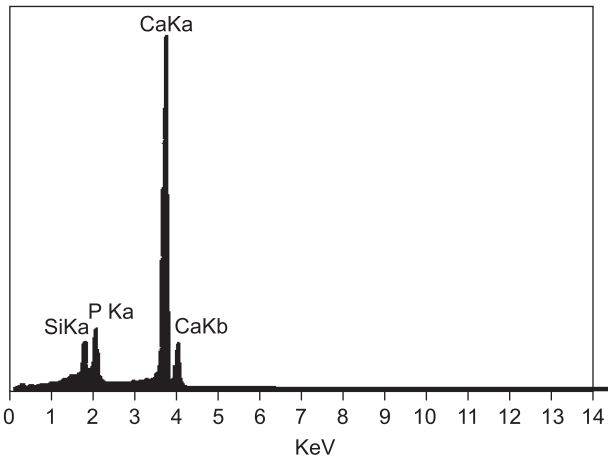

d) elemental micro-analysis of strut surface

Figure 3. SEM micrographs and EDS pattern of SH3.

Figure 4 shows the typical features of precipitation on SH0, SH1, and SH3 after immersing in SBF for 21 days. Deposition with the bone-like apatite morphology was occurred on all scaffolds after immersion in SBF. The morphology of precipitations was nearly similar among the scaffolds surfaces. The results from the EDX analysis confirmed the formation of an apatite layer on Scaffold after soaking in SBF (Figure 4b). Precipitation started at individual granules and the granules gradually grew together to form a dense layer on the specimen surface. High-magnification SEM images further revealed that each Ca–P granule consisted of a large number of tiny flake-like crystals. They were comprised of nano-crystals with the typical morphology of mineralized HA (Figure 4a and Figure 4c). Ca–P precipitations with similar morphology have been reported in previous studies [21, 22]. The SH1 and SH3 scaffolds exhibited a better ability of precipitation than that of SH0 (Figure 4d). The SH1 scaffolds in comparison with SH3 scaffolds exhibited a better ability of Ca–P formation. The ability of precipitation could be judged by the amount and size of granules. The size of granules on SH1 (Figure 4c) was much larger than that on other scaffolds. The ability of Ca–P formation or Ca–P induction *in-vitro* was semi-quantitatively compared by SEM examinations. The percentage of areas covered by Ca–P precipitation was evaluated from SEM micrographs for each type of sample. We noted a general trend of Ca–P formation capability: normal on SH0, good on SH3 and excellent on SH1.

From the above results, it could be concluded that the formation of crystalline phase (SiP_2O_7) during the sintering decreased the bioactivity while increased the mechanical property. This phenomenon is in well agreement with the results of other researchers [23].

CONCLUSION

This work successfully synthesized novel, highly porous, mechanically competent, and nanostructured bioactive glass-coated HA scaffolds for bone engineering. It was found that initially the minimum grain size of the coating increased from ~58 nm at 800°C to about 91 nm at 1000°C. A significant finding was that this simple method enhanced the compressive strength of porous

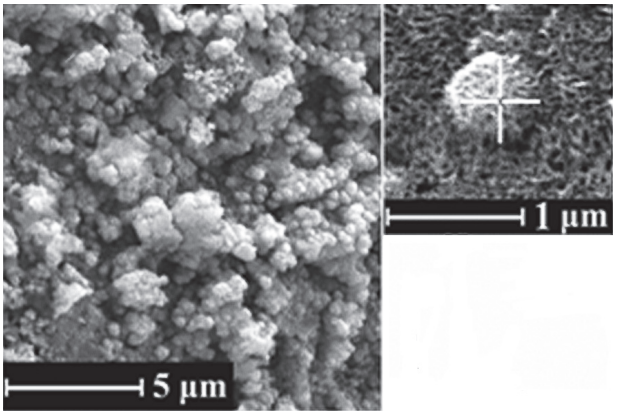

a) pore structure

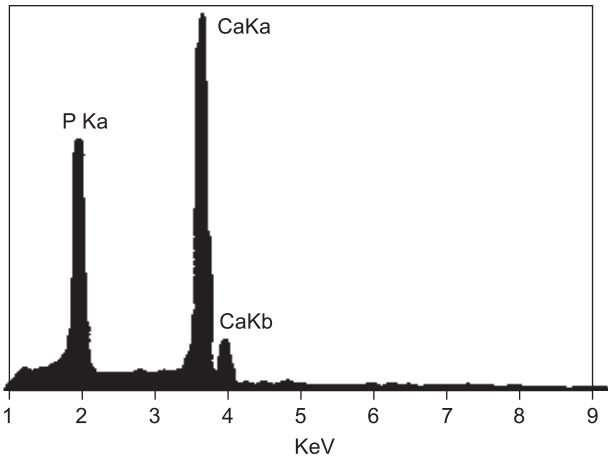

b) SH3

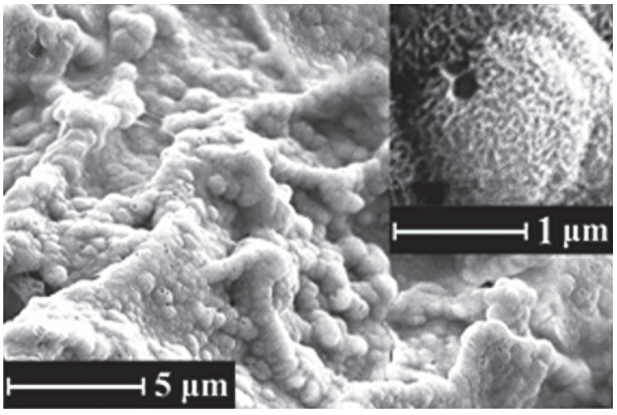

c) SH1

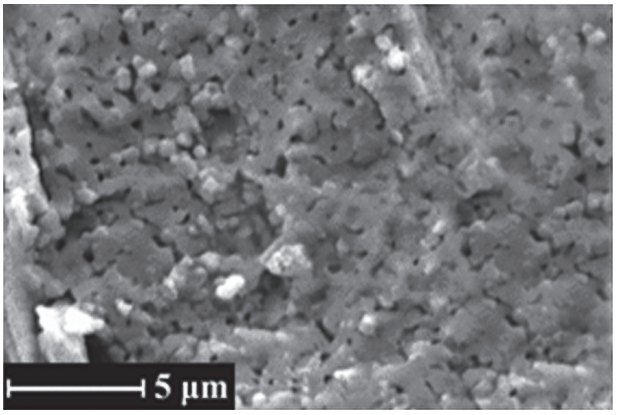

d) SH0

Figure 4. SEM micrographs of scaffold surfaces after 21 days of immersion in SBF.

HA from 0.22 to 1.49 MPa without using any polymeric materials. The compressive strength of scaffolds increased with increasing the sintering temperature. On the other hand, the in vitro bioactivity decreased with increasing the sintering temperature. SH1 scaffolds exhibited remarkable bioactivity along with suitable mechanical properties and may be a suitable candidate for bone tissue engineering.

References

1. Karp J.M., Dalton P.D., Shoichet M.S.: Mater.Res.Bull. *28*, 301 (2003).
2. Eggli P.S., Muller W., Schenk C.R.K.: Clin.Orthop.Relat. Res. *232*, 127 (1988).
3. Doblare M., Garcia J.M., Gomez M.J.: Eng.Fract.Mech. *71*, 1809 (2004).
4. Emadi R., Esfahani S.I.R., Tavangarian F.: Mater.Lett. *64*, 993 (2010).
5. Vallet-Reg M.: Dalton Trans. *44*, 5211 (2006).
6. Karageorgiou V., Kaplan D.: Biomaterials *26*, 5474 (2005).
7. Salgado A.J., Coutinho O.P., Reis R.L.: Macromol.Biosci. *4*, 743 (2004).
8. Kim H.W., Knowles J.C., Kim H.E.: J.Mater.Sci.Mater. Med. *16*, 189 (2005).
9. Kim H.W., Knowles J.C., Kim H.E.: Biomaterials *25*, 1279 (2004).
10. Tian T., Jiang D., Zhang J., Lin Q.: Mater.Sci.Eng.C *28*, 51 (2008).
11. Miao X., Lim G., Loh K.H.: Mater.Proc.Prop.Perf. *3*, 319 (2004).
12. Saravanapavan P., Hench L.L.: J.Biomed.Mater.Res. *54*, 608 (2001).
13. Cook R., Fielder E., Watson T., Robinson P., Hench L.L.: Bioceramics *13*, 625 (2000).
14. Hench L.L.: Curr.Opin.Solid.State.Mater.Sci. *2*, 604 (1997).
15. Kokubo T., Takadama H.: Biomaterials *27*, 2907 (2006).
16. Cullity B.D.: *Elements of X-ray Diffraction*, 2nd Edition, Addison-Wesley Publishing Company, Reading, MA, 1978.
17. Engin O., Tas A.C.: J.Eur.Ceram.Soc. *19*, 2569 (1999).
18. Clupper D.C., Hench L.L.: J.Non-Cryst.Solid *318*, 43 (2003).
19. Rohlmann A., Zilch H., Bergman G.: Arch.Orthop.Trauma. Surg. *97*, 95 (1980).
20. Gibson L., Ashby M.: Cellular solids structure and properties. 2nd ed. Cambridge University Press, New York: 1997.
21. Zhang Y.L., Mizuno M., Yanagisawa M., Takadama H.: J.Mater.Res. *18*, 433 (2003).
22. Guo L.H., Huang M., Leng Y., Davies J.E., Zhang X.D.: Key.Eng.Mater. *19*, 187 (2001).
23. Chen Q.Z., Thompson I.D., Boccaccini A.R.: Biomaterials *27*, 2414 (2006).